

# CFD-Based Redesign of a Low-Boom Supersonic Demonstrator Concept\*

Elwood Shields<sup>1</sup>

*Alliant Techsystems, Inc., Hampton, Virginia 23681, USA*

Wu Li<sup>2</sup>

*NASA Langley Research Center, Hampton, Virginia 23681, USA*

To design a more realistic low-boom supersonic demonstrator concept, theoretical engines were replaced with F-100 type engines. The original nacelle for the theoretical engine is replaced with a larger nacelle that is assumed adequate to house the F-100 engine. The process to redesign the configuration is then described and the rationales for design changes are given in some detail. Computational fluid dynamics (CFD) analysis was used to compute the equivalent area ( $A_e$ ) of the configuration during the redesign process. The goal of redesigning the configuration to match the CFD  $A_e$  of the configuration to a low-boom target was accomplished. The ground signature for CFD  $A_e$  of the redesigned configuration has similar low-boom characteristics as that of the original low-boom configuration with theoretical engines.

## Nomenclature

$A_e$  = equivalent area  
 $X_e$  = equivalent length

## I. Introduction

IT is generally accepted that the next generation of supersonic commercial aircraft will have to show the ability to produce a ground signature that is deemed acceptable to the general public in order to operate over land. To answer many of the questions that are associated with producing an acceptable ground signature, it is almost certain that some type of demonstrator aircraft will need to be built. In Ref. 1, a case study was performed to design a low-boom configuration that could be considered as a demonstrator concept. That configuration was designed for a start of cruise weight of 30,000 lb, a cruise Mach number of 1.6, a cruise altitude of 45,000 ft, and enough volume in the fuselage for a cockpit. The primary objective of the process was to develop a shaped signature on the ground with the lowest possible noise level measured in the perceived loudness (PLdB). The desired range of the supersonic cruise portion of the mission was 1000 nm. This configuration had a theoretical engine that was sized for the aircraft and was considerably smaller than most supersonic engines available today. To develop a more viable concept for a potential near-term flight demonstrator project, it is more cost effective and less risky to use a jet engine that is readily available. A version of the F-100 engine used in F-15s and F-16s would be a likely candidate for a demonstrator. This paper will document the redesign process to regain the low-boom characteristics for the demonstrator concept after replacing the theoretical engine with an F-100 engine concept. This process uses computational fluid dynamics (CFD) analysis in a mixed-fidelity design process<sup>2</sup> to efficiently match the configuration's equivalent area ( $A_e$ ) to a low-boom target and regain the low-boom characteristics that the original configuration has.

The CFD analysis results given in this paper were generated by an automated CFD analysis process<sup>3</sup> for conceptual design using Cart3d.<sup>4</sup> The mesh size for a Cart3d run is about 4 million cells and the analysis takes about 20 minutes on a computer cluster when using 48 processors (Intel Xeon CPU of 2.8GHz). The choice of using a

---

\* AIAA Paper for 29th AIAA Applied Aerodynamics Conference, June 2011, Honolulu, Hawaii.

<sup>1</sup> Senior System Engineer, Aeronautics Systems Analysis Branch, Space Division

<sup>2</sup> Senior Research Engineer, Aeronautics Systems Analysis Branch, Mail Stop 442

mesh of 4 million cells for CFD surface pressure analysis was based on a convergence study of the CFD  $A_e$  with respect to mesh size. The ground signatures in this paper are calculated by using sBOOM<sup>5</sup>, a sonic boom analysis code that uses the augmented Burgers equation to propagate  $A_e$  or off-body pressure distributions to the ground.

The paper is organized as follows: Section II describes the F-100 engine selection, the corresponding nacelle definition, and the analysis of a new baseline configuration using the conceptual F-100 nacelles. The CFD  $A_e$  matching process for redesign of the low-boom demonstrator concept is documented in section III and the concluding remarks are given in section IV.

## II. Baseline Configuration with an F-100 Engine Concept

The F-100 type engine was selected as a good candidate for a demonstrator concept because more than 7000 have been built and installed in supersonic aircraft, specifically F-15 and F-16 fighter jets. These engines have been very reliable over several years and appear to have more than enough thrust for the demonstrator concept.

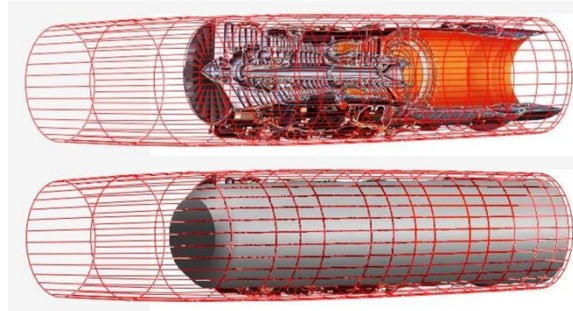


Figure 1. The conceptual engine, internal diagram, and nacelle for F-100



Figure 2. Comparison of the original and F-100 nacelle shapes

Packaging of engines in nacelles at the conceptual level is usually not all that rigorous, because the engines that are used are also conceptual and not well defined in terms of size and shape. The conceptual engine is usually represented by a simple solid body that is assumed large enough to accommodate not only the engine but all the accessories and plumbing that are not described in great detail at this point in the design process. In this study, the F-100 engine was modeled as a conceptual engine. A solid body that represents an F-100 engine was created using published numbers. The conceptual F-100 engine has a length of 191 inches and a diameter of 34.8 inches at the fan face. The diameter of the engine increases linearly to a maximum diameter of 46.5 inches at the location of 10 inches aft of the fan face and retains that diameter for the remainder of the length. This conceptual engine model is consistent with the level of detail at the conceptual design phase. A nacelle was created around this solid body. Using a standard rule of thumb, the nacelle was extended by 70 in (twice the length of the engine inlet diameter) in length ahead of the engine face to account for an axi-symmetric supersonic inlet and increased by eight inches in the maximum diameter to account for the yet to be defined structure, accessories and plumbing. The initial F-100 nacelle is 264 inches in length and has a maximum diameter of 58 in. The conceptual engine as a solid body and a diagram representing the F-100 engine are both shown in Fig. 1 along with the initial conceptual F-100 nacelle shape. Figure 2 shows a comparison of the shapes of the original (red) and F-100 (gray) nacelles.

The original demonstrator concept described in Ref. 1 was designed to match a low-boom  $A_e$  target that resulted in a shaped ground signature (see Figs. 3 and 4). After completion of the original case study, additional small changes to the configuration were made in an effort to achieve an improved  $A_e$  match and lower PLdB ground signature. These intermediate efforts did not result in any significant improvements to the  $A_e$  matching or to the ground signature. The redesign effort documented here used this slightly revised configuration for the starting point for which the original conceptual nacelles were replaced with the conceptual F-100 nacelles.

The results in Fig. 5 show that there is a significant change in the  $A_e$  distribution with the new nacelles. Not only is the volume change reflected in the results, but also the shocks from the larger nacelles have an impact on the other components of the configuration including the wing and horizontal tail, resulting in a change to the lift distribution

of the entire configuration. Figure 6 shows the resulting ground signature. The differences in the shock patterns can be seen in Fig. 7 which shows the pressure contours of the original configuration and the new baseline with the F-100 nacelles.

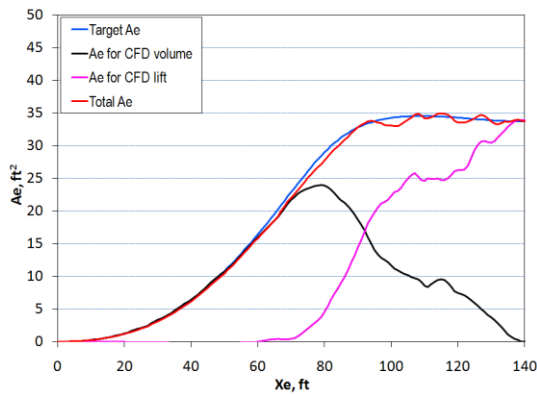


Figure 3. CFD  $A_e$  for the original configuration

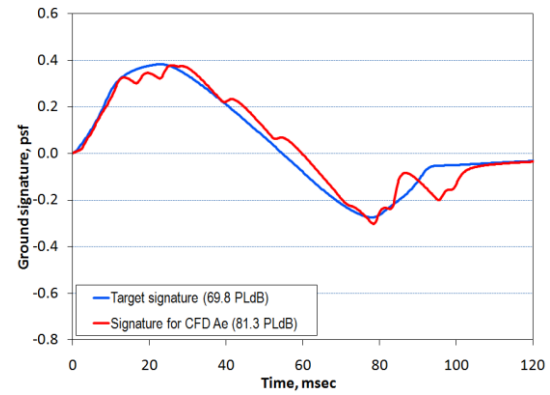


Figure 4. Ground signature for the original configuration

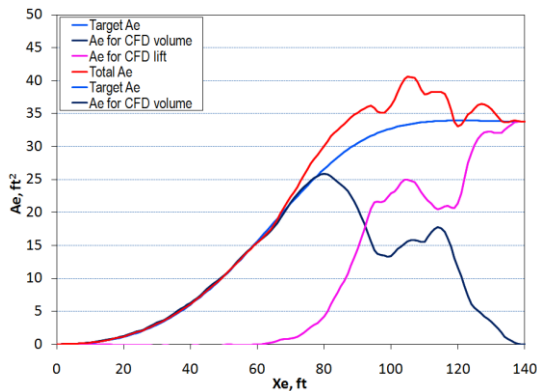


Figure 5. CFD  $A_e$  for modified configuration



Figure 6. Ground signature for modified configuration

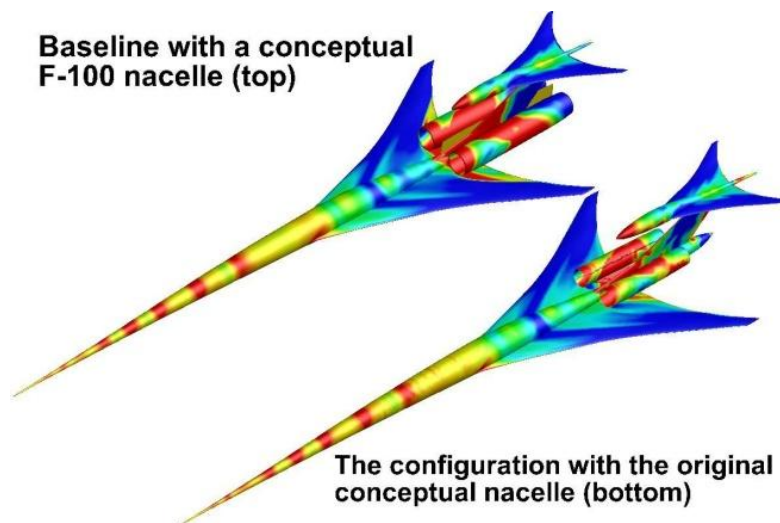


Figure 7. Surface pressure contours of two configurations

### III. CFD-Based Redesign Process of Demonstrator Concept

In this section, we document the CFD-based redesign process of matching the configuration's  $A_e$  to a low-boom target, including the choice of a feasible low-boom target, the configuration changes that were made in an attempt to match the low-boom target  $A_e$ , and rationales for design changes.

Even though an initial effort was made to reduce the gap between the configuration's  $A_e$  and the low-boom target by changing the fuselage volume using BOSS<sup>6</sup> (a shape optimization code for low-boom design), it was fairly obvious that there was insufficient volume in the fuselage to accomplish this task as the cross-sectional area of the fuselage would shrink to zero at some locations. Other geometry modifications were then considered including wing planform changes and changes to the shapes and locations of the tail surfaces, nacelles, pylons and pod. These modifications were inadequate in reducing the difference between the  $A_e$  of the configuration and the low-boom target to a level where the remaining differences could be eliminated by fuselage and pod shaping with BOSS or using interactive geometry modeling tools.

As a result, the decision was made to increase the cruise weight to 36,000 lb for a number of reasons. First, this would allow for a new  $A_e$  target to be created with more area available for the fuselage when minimizing the  $A_e$  mismatch. Second, because the F-100 engines are heavier than the original conceptual engines, it is not unreasonable to assume that the configuration would be heavier. Third, this increase would also allow more fuel for the supersonic cruise portion of the mission which was an issue at the cruise weight of 30,000 lb. Preliminary performance calculations showed that a start of cruise weight of 36,000 lb will allow the configuration to approach the desired supersonic cruise range of 1000 nm.

A CFD analysis of the configuration was performed at the cruise weight of 36,000 lb. The  $A_e$  analysis results for the 36,000 lb baseline configuration are compared in Fig. 8 with a new 36,000 lb  $A_e$  target. The corresponding ground signature and new target signature are shown in Fig. 9. The new target was developed using the parametric  $A_e$  target explorer.<sup>1</sup> The new target allows for more volume in the configuration while keeping the PLdB of the corresponding ground signature virtually the same as the original ground signature. In general, at each iteration of the redesign process, there is an opportunity to redefine the  $A_e$  target if this would lead to a low-boom target that is easier to match. Such changes to the low-boom  $A_e$  target were made during the redesign process as shown later.

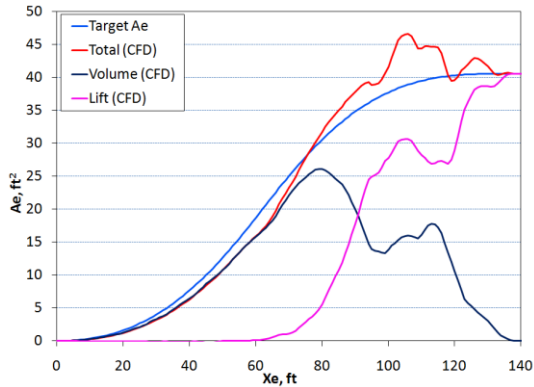


Figure 8. CFD  $A_e$  for cruise weight of 36,000 lb

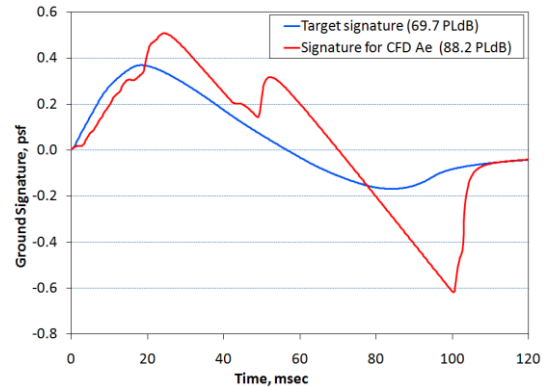


Figure 9. Ground signature for cruise weight of 36,000 lb

As shown in Fig. 8, a deficiency of  $A_e$  forward of  $X_c = 75$  existed while there still was an excess of  $A_e$  in the aft portion ( $X_c > 75$ ) of the distribution. The forward deficiency could be filled by increasing the fuselage volume, a forward shift of the lift distribution, or a combination of the two. The aft portion gap still appeared too large for volume changes alone and would require changes to the lift distribution to minimize the gap. The forward gap was addressed first and planform changes were made in an effort to at least partially close the gap with a change in the configuration's lift distribution. The planform that was eventually adopted added area forward by increasing the leading edge sweep to 82.5 degrees for the first 6 percent of the exposed wing span and increasing the notch ratio slightly by increasing the trailing edge sweep by approximately 2 degrees. There was also an increase to the span of about one foot and a change in the sweep at the tip of about 8 degrees. This latter change was done more for performance than for sonic boom mitigation. These changes did result in a small reduction in the gap in the forward portion of the  $A_e$  distribution but fell well short of eliminating the forward gap. The planform changes were however retained as the design process moved forward because they did have a small positive effect on both the  $A_e$  gap and the overall performance of the configuration. The remaining forward  $A_e$  gap was filled by increasing the fuselage volume using BOSS. Increasing the fuselage volume was not as much of an issue as decreasing it because the

starting fuselage volume was near what was considered a minimum. These changes can be seen in the top plot of Fig. 10.

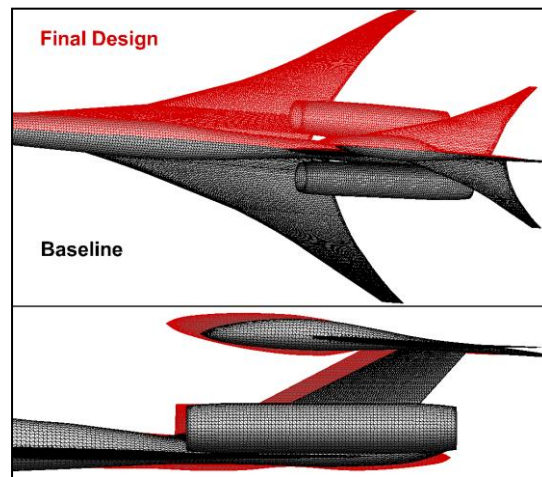


Figure 10. Shape comparison

The next item addressed was the large amount of  $A_e$  still above the target in the aft portion of the distribution that cannot be removed by decreasing the configuration's fuselage or pod volume. A change in the configuration's lift distribution appeared to be the next viable alternative. This could be accomplished in different ways but virtually all of them would require more lift to be carried on the horizontal tail. Because the total lift was fixed at 36,000 lb, adding lift to the horizontal tail will obviously take lift away from the wing. This decrease in the  $A_e$  due to the wing lift needed to be in the aft portion of the wing where the impact of the F-100 nacelles causes the greatest gap between the configuration's  $A_e$  and the target. It was decided to accomplish this with an increase to the incidence of the horizontal tail because this appeared to be the simplest way to determine if shifting lift from the wing to the tail would yield the desired results. Because there are other changes to the overall lift distribution when the lift on the tail is changed, a minimal change of the incidence is desirable. After an increase in the tail incidence of one degree, the difference between the configuration's  $A_e$  and the target for  $X_e < 120$  became manageable with volume changes to the fuselage and pod. It should be noted that early in the design process, when it was initially decided to carry more lift on the horizontal tail, the planform of the tail was chosen to be the same as that of the wing. This was done so that it would be an efficient lifting surface and hopefully would not have a significant impact on the performance of the configuration. The decision to put even more lift on the tail, however, results in a greater impact to the performance and raises the level of concern about structural feasibility and stability and control of the configuration, which we do not address in this paper.

The resulting  $A_e$  distribution of the configuration now had an area where it was below the target  $A_e$  in the portion of the distribution around  $X_e = 120$ . By moving the pod forward, this could be addressed with pod volume and possibly horizontal tail lift. In order to keep the pod from being too far forward on the vertical tail, the vertical tail was also moved forward the same amount. See the bottom plot of Fig. 10. These changes required further  $A_e$  refinement using BOSS and interactive shaping with the geometry modeling tools. This modification led to a better match of the  $A_e$  for all but the portion of the  $A_e$  distribution where  $X_e > 120$ . This portion of the distribution is almost completely driven by the horizontal tail and the pod. The first efforts of minimizing this  $A_e$  gap were accomplished by changing the pod volume and to some extent changing the location of the pod. It is much more intuitive to change volume than lift because the result of volume changes is more local to the portion of the  $A_e$  distribution in question. Changing lift on the tail also changes the lift of the wing because we hold the cruise weight constant and this leads to changes on a much greater portion of the  $A_e$  distribution. The resulting changes led to a larger pod volume in the front portion, and a rapid decrease in volume from about the midpoint to the end. See Fig. 10 for the pod shape changes.

At this point, the above modifications were successful in reducing the  $A_e$  gap, however, it actually made the PLdB of the ground signature slightly worse. Another adverse impact was the creation of an area of positive pressure on the horizontal tail where the pod volume decreased quickly resulting in a reduction in performance. It was then decided that some change would need to be made to the horizontal tail lift distribution. Like so many of the changes in this process, the lift change can be made in a number of ways including changes to the incidence angle, planform shape, location of the tail, or camber and twist. Changing the incidence would put more lift on the tail but



would not accomplish the complicated redistribution of the lift in the region of  $X_e > 120$  to eliminate the  $A_e$  mismatch. Changing the camber or twist should change the distribution but could also have a negative effect on the performance. It was decided to change the planform in an effort to not only move the tail lift forward but also to change the lift distribution for  $X_e > 120$ . Figure 11 shows three different horizontal tail planforms. The blue tail was the original planform and the red planform was the first attempt. This change moved the tail lift forward but then caused a significant negative gap in the total  $A_e$  behind where the original positive gap was. The green planform is between the red and the blue and is a compromise that left two small gaps on both sides of the original aft gap but decreased the PLdB value of the ground signature.

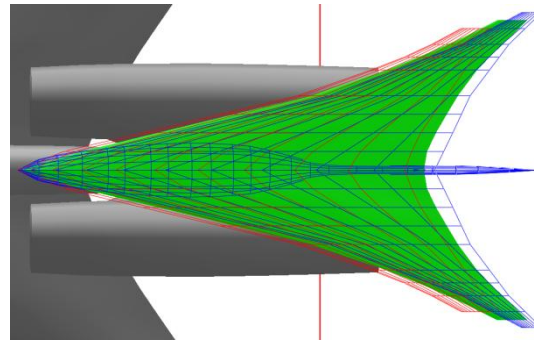


Figure 11. Tail planform changes

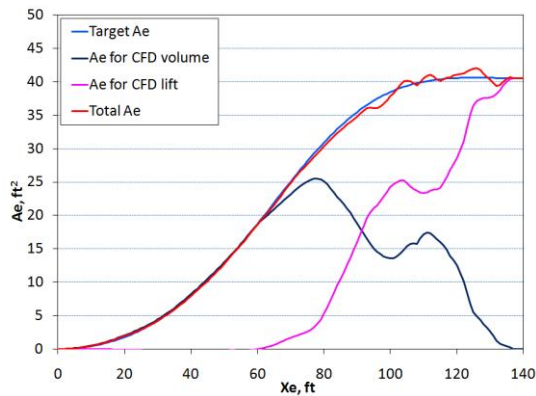


Figure 12. CFD  $A_e$  for cruise weight of 36,000 lb

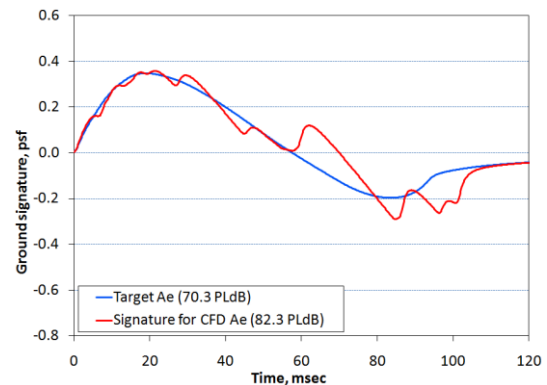


Figure 13. Ground signature for cruise weight of 36,000 lb

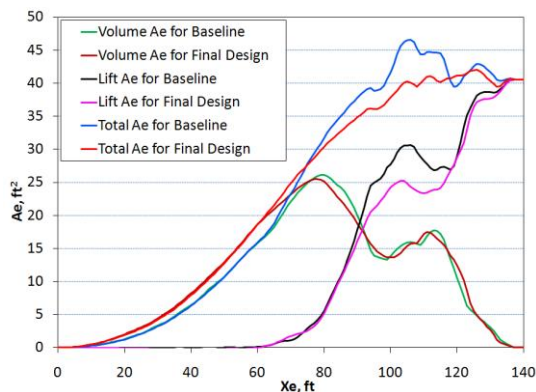


Figure 14. CFD  $A_e$  comparison of baseline and final designs

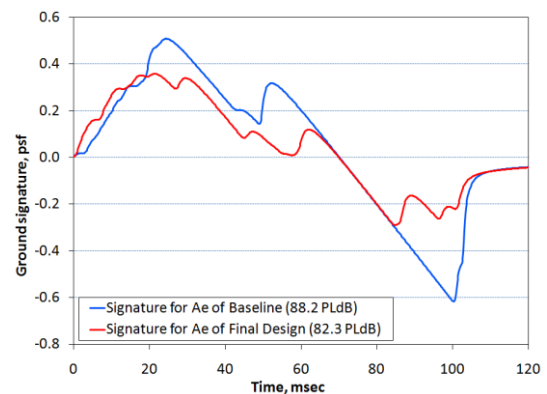


Figure 15. Ground signature comparison of baseline and final designs

Figure 12 shows the final results of the redesign process to match a low-boom  $A_e$  target and Fig. 13 shows the resulting ground signature. Note that the initial  $A_e$  target in Fig. 8 is different from the final  $A_e$  target in Fig. 12 as

shown by the different PLdB values of the corresponding ground signatures in Figs. 9 and 13. A comparison of the CFD  $A_e$  distributions from the final design and the baseline are shown in Fig. 14 and a comparison of the ground signatures are shown in Fig. 15. The pressure contours of the baseline and final configurations are shown in Fig. 16.

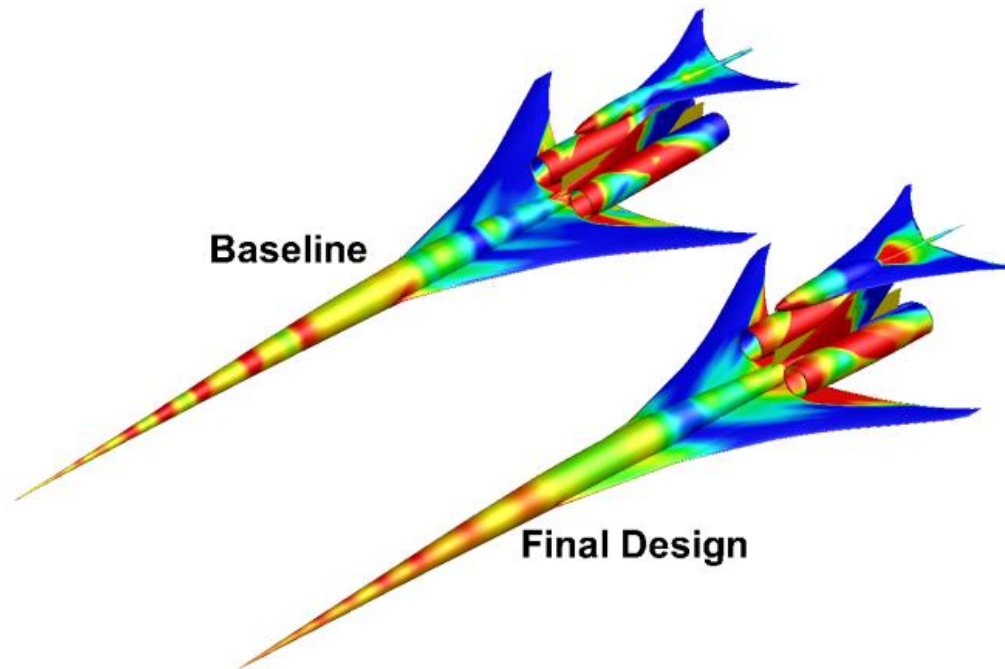


Figure 16. Surface pressure contours of the baseline and the final design

A careful review of Fig. 10 will reveal that there are other changes to the configuration that have not been described in any detail. An example is that the nacelles are moved forward. This was just one more effort to fill a gap between the configuration's  $A_e$  and the target. Although this change seemed reasonable at the time, and to some extent may have accomplished what could be described as a better  $A_e$  match, it actually had little or no effect in the end on the ground signature shape and its PLdB value. At this point it was decided that this process had accomplished the goal of integrating larger more realistic nacelles that would house F-100 type engines and regaining a ground signature that has similar low-boom characteristics to that of the initial configuration with the smaller nacelles.

#### IV. Concluding Remarks

The task of replacing a theoretical engine with an F-100 engine concept, redesigning the configuration to regain the low-boom characteristics of the original configuration was accomplished successfully. During the redesign process, more than fifty computational fluid dynamics (CFD) analyses were completed and each one was preceded by some design changes that were based to some extent on past experiences and the preceding CFD analysis results. The path taken in this process is not unique to accomplishing the goal, but it does show that the tools now available to a designer allow for a much more comprehensive design study utilizing a much larger and more accurate set of data during the early conceptual design phase. The resulting low-boom design based on CFD equivalent area analysis can be used as the starting point of a design process that uses CFD off-body pressure distribution for boom analysis to obtain a configuration with a fully shaped ground signature.<sup>7</sup>

#### Acknowledgment

The authors would like to thank Jim Fenbert, Karl Geiselhart, and Lori Ozoroski for many instrumental comments on earlier versions of this paper.

## References

- <sup>1</sup> Li, W. and Shields, E., “Generation of Parametric Equivalent-Area Targets for Design of Low-Boom Supersonic Concepts,” AIAA-2011-462, January 2011.
- <sup>2</sup> Li, W., Shields, E., and Geiselhart, K., “A Mixed-Fidelity Approach for Design of Low-Boom Supersonic Aircraft,” AIAA-2010-0845, January 2010. (accepted for publication in *Journal of Aircraft*)
- <sup>3</sup> Ordaz, I., and Li, W., “Integration of Off-Track Sonic Boom Analysis in Conceptual Design of Supersonic Aircraft,” AIAA-2011-464, January 2011.
- <sup>4</sup> Aftosmis, M., “Cart3D Resource Website,” <http://people.nas.nasa.gov/~aftosmis/cart3d/cart3Dhome.html> [cited May 2011].
- <sup>5</sup> Rallabhandi, S., “Advanced Sonic Boom Prediction Using Augmented Burger's Equation,” AIAA-2011-1278, January 2011.
- <sup>6</sup> Li, W., Shields, E., and Le, D., “Interactive Inverse Design Optimization of Fuselage Shape for Low-Boom Supersonic Concepts,” *Journal of Aircraft*, Vol. 45, No. 4, 2008, pp. 1381–1398.
- <sup>7</sup> Li, W., and Rallabhandi, S., “Inverse Design of Low-Boom Supersonic Concepts Using Reversed Equivalent Area Targets,” AIAA paper no. pending, June 2011.